

Seeing Hofstadter's Butterfly in Atomic Fermi Gases

Lei Wang and Matthias Troyer

Theoretische Physik, ETH Zurich, 8093 Zurich, Switzerland

We propose a novel way to detect the fractal energy spectrum of the Hofstadter model from the density distributions of ultracold fermions in an external trap. At low temperature, the local compressibility is proportional to the density of states of the system which reveals the fractal energy spectrum. However, thermal broadening and noises in the real experimental situation inevitably smear out fine features in the density distribution. To overcome this difficulty, we use the maximum entropy method to extract the density of states directly from the noisy thermal density distributions. Simulations show that one is able to restore the core feature of the Hofstadter's butterfly spectrum with current experimental techniques. By further reducing the noise or the temperature, one can refine the resolution and observe fine structures of the butterfly spectrum.

PACS numbers: 67.85.Lm, 51.35.+a, 71.20.-b, 73.43.-f

The Hofstadter model [1] describes electrons moving in a 2D lattice exposed to a uniform magnetic field, where the interplay of lattice potential and magnetic field leads to an intriguing fractal energy spectrum, called Hofstadter's butterfly. Being one of the first quantum fractals discovered in nature, Hofstadter studied it around the same time when Mandelbrot coined the term "fractal".

Despite its mathematical beauty, Hofstadter's butterfly remained elusive for decades, because it requires infeasibly strong magnetic fields to see in the conventional crystals. Attempts have thus been made in artificial superlattices, where much smaller magnetic fields suffice. Early experiments reported signatures for the fractal spectrum in the 2D electron gas with a weak lateral superlattice potential [2] and recently more evidence was reported for graphene superlattices [3–5]. Since the system realizes a quantum Hall insulator when the chemical potential is in the energy gaps [6], these solid state experiments utilize the Hall conductance as a probe [7] of the butterfly.

Hofstadter's butterfly is also a long sought goal [8–14] in cold atoms systems ever since the original proposal [15]. Cold atomic gases offer a unique chance to study the model in the absence of disorder and with tunable interactions. Recently, two groups reported the realization of Hofstadter's model in optical lattices [16, 17], using laser-assisted tunneling to imprint complex phases to the hopping amplitudes and verifying the induced flux by studying the dynamics of bosons in the lattice. A natural next goal is the definite observation of Hofstadter's butterfly in an optical lattice. However, contrary to solid state setups [2–5], measuring the Hall conductance of the ultracold Fermi gases is not straightforward [18–22].

In this Letter, we thus propose a simple and novel way to measure Hofstadter's butterfly from the simplest thermodynamic quantity, the density distribution of the trapped Fermi gases. At low temperature the local compressibility is equal to the density of states (DOS), which directly reveals the fractal energy spectrum. However, in experiments thermal fluctuations inevitably smear out

the fine features in the density distribution. We thus propose to use the maximum entropy method [23] to extract the DOS from the noisy finite temperature density distributions. Our simulations show that one is able to recover Hofstadter's butterfly solely from in situ imaging of the density profiles at current achievable temperature and resolution.

The Hamiltonian of the Hofstadter model reads,

$$H = -J \sum_{m,n} e^{-i2\pi n\phi} \hat{c}_{m+1,n}^\dagger \hat{c}_{m,n} + \hat{c}_{m,n+1}^\dagger \hat{c}_{m,n} + H.c., \quad (1)$$

where J is the hopping amplitude and $\hat{c}_{m,n}$ are the fermionic annihilation operator, with m and n being the column and row indices of a square lattice. An atom hopping clock wise around a plaquette on the square lattice accumulates a phase ϕ . Since the typical temperature in the optical lattice is higher than the energy scales associated with the fractal energy spectrum, it is essential to consider the finite temperature properties of the model. To calculate the thermodynamic properties, we adopt the exact diagonalization (ED) [24] and the quantum transfer matrix method (QTM) [25, 26]. In both methods we choose $\phi = p/q$ where p, q are two relatively prime integers. In the ED calculation, we diagonalize the Bloch Hamiltonian for each momentum and then calculate the thermodynamical quantities from the exact energy spectrum. In the QTM approach, we calculate the partition function of a system with fixed width and let the length grow to infinite. All other thermodynamic quantities can then be calculated from numerical differentiation of the grand-canonical thermodynamical potential. We have cross checked the results from both methods.

The key physical observable is the density versus chemical potential, which is related to the DOS $D(\varepsilon)$ through

$$\rho(\mu, T) = \int_{-\infty}^{\infty} f\left(\frac{\varepsilon - \mu}{k_B T}\right) D(\varepsilon) d\varepsilon, \quad (2)$$

where $f(x) = 1/(e^x + 1)$ is the Fermi-Dirac distribution, T is temperature of the system. To probe the DOS, we

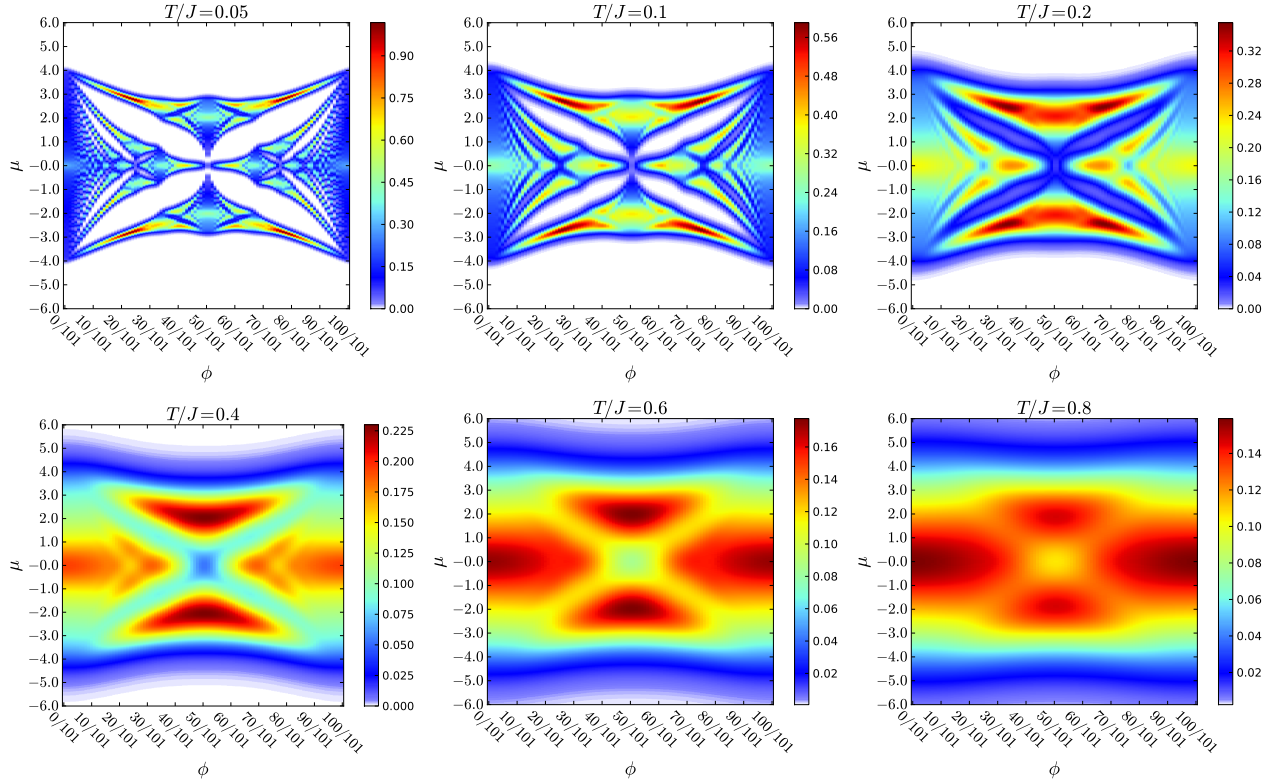


Figure 1: The compressibility of the Hofstadter model versus the chemical potential μ and flux ϕ at different temperatures.

take a derivative of both sides and get the compressibility

$$\kappa(\mu, T) \equiv \frac{\partial \rho}{\partial \mu} = \int_{-\infty}^{\infty} \frac{\partial f}{\partial \mu} D(\varepsilon) d\varepsilon. \quad (3)$$

Since $\partial f / \partial \mu = f(1-f)/(k_B T)$ approaches to the Dirac delta function $\delta(\varepsilon - \mu)$ at zero temperature, the zero temperature compressibility directly probes the DOS [47]:

$$D(\varepsilon) = \lim_{T \rightarrow 0} \kappa(\varepsilon, T). \quad (4)$$

Figure 1 shows the compressibility versus chemical potential and magnetic flux at different temperatures. At $T/J = 0.05$ one can clearly see the fractal shape of the energy spectrum. The compressibility is zero when the chemical potential is in the energy gap. At higher temperature the fine features in the compressibility are smeared out, but the coarse feature of the butterfly remains. Even at $T/J = 0.8$, the suppression of the compressibility close to $\mu = 0, \phi = 1/2$ is still visible. There the system has Dirac like dispersion around $\mu = 0$ and the DOS vanishes linearly. This is in contrast to the $\phi = 0$ case where the compressibility peaks at $\mu = 0$ because of the Van Hove singularity in the DOS.

In cold atom experiments the trapping potential provides a scan of the chemical potential which can be

used to determine the density of states of a uniform system [48]. To see this we first treat the trapping potential using a local density approximation (LDA). The local chemical potential varies as $\mu(r) = \mu_0 - \alpha r^2$ where μ_0 is the chemical potential in the trap center, α is related to the geometric mean of the trapping frequencies and the atom mass, r is the rescaled distances of a site to the trap center. The density $\rho(r)$ can be measured from the in situ imaging of the atomic cloud [27–30]. The local compressibility can then be estimated as

$$\kappa(r) = -\frac{1}{2\alpha r} \frac{d\rho}{dr}. \quad (5)$$

Combining this with the known $\mu(r)$ one can recover $\kappa(\mu)$ up to an overall shift of the chemical potential. Collecting measurements for different ϕ , one can then recover the compressibility plots shown in Fig. 1 [49].

Finite temperature effects and sampling noise inevitably smear out the fine features in the density profile in experimental measurements. Noisy signals pose problems for extracting the local compressibility from the density distributions, which raises the question whether is it possible to observe the fractal structure of κ at an experimental accessible temperature. Figure 2(a) shows results for $N = 60000$ fermions in a three-dimensional (3D) trap with $\alpha = 0.006, \phi = 1/3$ and entropy per particle $S/N = 1.0k_B$, which is currently easily accessible [31]. It corresponds to a temperature $T/J = 0.873$ and the fine

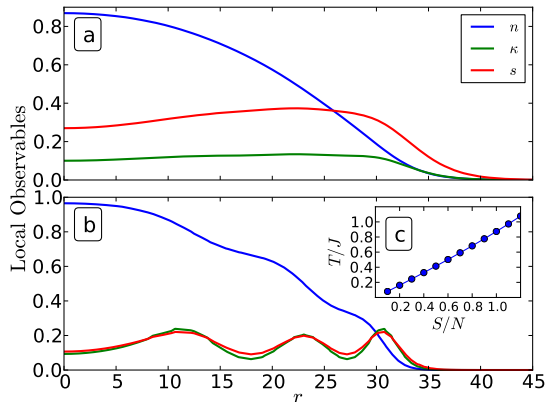


Figure 2: **Local observables in a 3D harmonic trap.** Solid lines show the density ρ , compressibility κ and entropy s with $N = 60000$, $\alpha = 0.006$ and $\phi = 1/3$. The entropy per particle is (a) $S/N = 1.0k_B$ and (b) $S/N = 0.4k_B$. The corresponding temperatures is $T/J = 0.873$ and $T/J = 0.329$ respectively. (c). The temperature of the cloud versus entropy per particle S/N calculated using LDA with the equation of state given by the quantum transfer matrix method.

features in local observables has been smeared out. Only when the entropy per particle is reduced to $S/N = 0.4k_B$ (Fig 2(b)), one can directly observe the density plateaus and the corresponding peaks in the local compressibility. To resolve a particular feature in the energy spectrum requires the temperature to be smaller than the corresponding energy gap. Figure 2(c) shows the temperature in unit of J versus the entropy per particle. The required entropy for resolving the plateau at $\phi = 1/3$ is comparable to achieving the antiferromagnetic states in the 3D Hubbard model [32], which is already a challenging task. Above analysis show that even without any noise, the thermal broadening effect already makes it difficult to resolve the Hofstadter butterfly from the local compressibility at experimentally achievable temperatures.

We now come to the key idea of this paper: one is nevertheless able to restore the density of states $D(\varepsilon)$ from a seemingly featureless and noisy thermal density distribution using techniques of spectral analysis. Knowing the temperature of the system (which we will discuss in the following), one can directly deconvolute the effect of the Fermi-Dirac distribution in the Eq.(2) or Eq.(3) to get $D(\varepsilon)$ from the density distributions. The zero temperature compressibility detection discussed above is a limiting case where one trivially deconvolutes a Dirac delta function in Eq.(3).

At high temperature it is in general difficult to deconvolute Eq.(2) as it is an ill-posed problem, especially given the experimental uncertainties in the measured equation of state $\rho(\mu)$. To solve the difficulty, the maximum entropy method [23] treats $D(\varepsilon)$ as a probability distribution and searches for the best solution

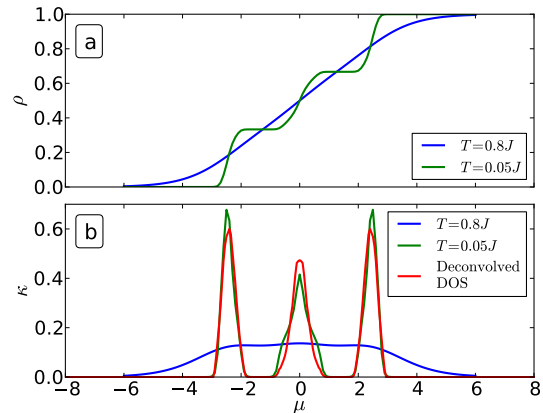


Figure 3: **Deconvolve the thermal broadening effect.** (a). Density ρ versus chemical potential μ at high ($T = 0.8J$) and low ($T = 0.05J$) temperatures, $\phi = 1/3$. (b). The corresponding compressibilities which at low temperature ($T = 0.05J$) reveals the DOS of the system. The red line shows the DOS restored from the $T = 0.8J$ density distribution using the maximum entropy algorithm.

(in the Bayesian sense) that is consistent with the measured data. The stochastic inference approach [33–36] employs a stochastic process and represents the resulting spectrum as an ensemble average of many feasible solutions. Recently, a new method based on the consistent constraints was also been proposed [37]. These methods have been used for the analytical continuation from the imaginary time quantum Monte Carlo data to the real frequency spectral functions [23, 38]. The deconvolution of Eq.(2) is related to the analytical continuation by setting the imaginary time $\tau = 0^-$ and introduce chemical potential dependence to the imaginary time Green's function.

We first apply the maximum entropy approach [50] to a noiseless high temperature density distributions and show it is able to deconvolute the thermal broadening effect. Figure 3(a) shows $\rho(\mu)$ at $T/J = 0.8$ which seems featureless compared to the density at $T/J = 0.05$. Figure 3(b) shows the corresponding compressibilities, where the one at $T/J = 0.05$ approximates the exact DOS well while the $T/J = 0.8$ one is much broader. Nevertheless, the deconvoluted DOS from the density at $T/J = 0.8$ agrees well with $\kappa(T = 0.05J)$, Figure 3(b). In particular, from the seemingly featureless density profile at high temperature, we have restored the three peaks in the DOS, corresponding to the three energy bands at $\phi = 1/3$.

To mimic noisy experimental measurements, we generate Gaussian distributed random numbers with standard deviation $\sqrt{\kappa T}$ according to the fluctuation-dissipation theorem (FDT) [39–41] and add them to the exact $\rho(\mu)$ data. We then feed the average values and statistical errors of 100 noisy samples (Fig.4) to the maximum en-

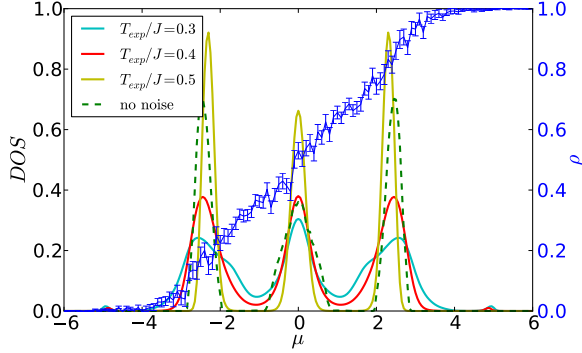


Figure 4: **Restoring the DOS from noisy data and imperfect temperature measurement.** The blue line with errorbars show the density profile at $T/J = 0.4$ with noises following the fluctuation-dissipation theorem. The three solid lines (cyan, red and yellow) show DOS restored from the noisy data using temperature $T_{exp}/J = 0.3, 0.4$ and 0.5 in the Fermi-Dirac kernel. The dashed green line shows the DOS restored from the exact $\rho(\mu)$ data.

trophy calculation. Random noise further washes out the fine features in the density and the resulting DOS are broader than the exact one. (compare in Fig.4 the red solid line against the dashed green line.) Nevertheless, the deconvoluted DOS based on the noisy data still correctly restores the three peaks correspond to the $\phi = 1/3$.

To determine the integral kernel $f(\frac{\varepsilon - \mu}{k_B T})$ one needs to determine the temperature T of the system, which can be done using several approaches [31]. In particular, when the density profile is available, one could fit the density in the wing of the cloud [42] (with theoretical input about the $\rho(\mu)$ in the dilute limit) or using the FDT [27, 39, 43] to determine the temperature. We examine the effect of error in the measured temperature T_{exp} on the restored DOS in Fig.4. If $T_{exp} > T$, the deconvolution results in a sharper DOS and the peak position are shifted, while $T_{exp} < T$ has the opposite effect. Still, the error in the measured temperature $T_{exp} \neq T$ does not destroy the overall feature of the DOS. This analysis also shows that the deconvolution is stable against small variations of temperature in different experimental runs.

Finally, we show the deconvoluted DOS at $T/J = 0.4$ and 0.8 with different ϕ in the Fig. 5(a-b). To further incorporate corrections beyond the local density approximation (LDA) [51], we use exact densities on a 101^2 lattice in a trapping potential with $\alpha = 0.006$. The deconvoluted DOS reproduces the butterfly spectrum at both temperatures, although the fine structures around the edge ($\phi \sim 0$ and $\phi \sim 1$) are smeared out. Figure 5(c-d) shows the DOS restored from noisy density data. Even at high temperature $T/J = 0.8$ one can still observe the reminiscent of the butterfly spectrum, where the suppression of $D(\mu = 0)$ at $\phi = 1/2$ compares to the $\phi = 0$ case is the most significant feature. By further decreas-

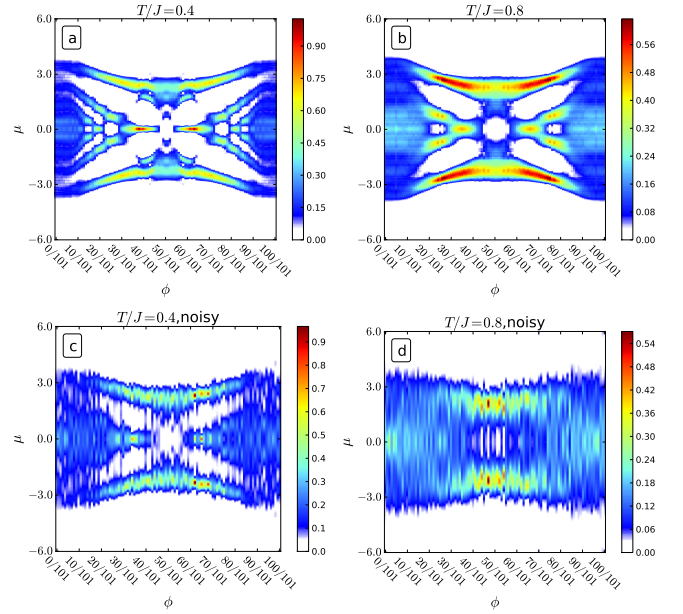


Figure 5: **The deconvoluted Hofstadter spectrum using thermal density distributions.** (a-b) without noises (infinite samples). (c-d). obtained from 100 noisy samples.

ing the temperature (Fig. 5(c)), one can uncover finer structures of Hofstadter's butterfly. More importantly, our simulation shows that it is more favorable to gather better statistics, which already allows one to restore the core feature of Hofstadter's butterfly (Fig. 5(b)) at high temperature ($T = 0.8J$). This is encouraging news for experimentalists who want to observe the butterfly spectrum.

In a broader context, our work provides an example of how spectral information can be extracted from static thermodynamic properties (the equation of state). In the context of this paper, a maximum entropy analysis of the noisy finite temperature density profiles turns out to yield sufficient information to allow observation of the Hofstadter butterfly in ultracold atomic Fermi gases. This approach can also be used in free space and other complicate optical lattices structures, to reveal the novel Dirac dispersions and flat bands [44, 45]. A generalization of our method to interacting systems would be of great interest.

Acknowledgment We thank Jakub Imřiška, Daniel Greif and Hiroshi Shinaoka for useful discussions. The work was supported by the Swiss National Science Foundation through the NCCR QSIT, the European Research Council, and the Aspen Center for Physics under National Science Foundation grant number 1066293. Simulations were performed on the Brutus cluster at ETH Zurich.

-
- [1] D. R. Hofstadter, *Phys. Rev. B*, **14**, 2239 (1976).
- [2] C. Albrecht, J. Smet, K. von Klitzing, D. Weiss, V. Umansky, and H. Schweizer, *Phys. Rev. Lett.*, **86**, 147 (2001).
- [3] C. R. Dean, L. Wang, P. Maher, C. Forsythe, F. Ghahari, Y. Gao, J. Katoch, M. Ishigami, P. Moon, M. Koshino, T. Taniguchi, K. Watanabe, K. L. Shepard, J. Hone, and P. Kim, *Nature*, **497**, 598 (2013).
- [4] B. Hunt, J. D. Sanchez-Yamagishi, A. F. Young, M. Yankowitz, B. J. LeRoy, K. Watanabe, T. Taniguchi, P. Moon, M. Koshino, P. Jarillo-Herrero, and R. C. Ashoori, *Science*, **340**, 1427 (2013).
- [5] L. A. Ponomarenko, R. V. Gorbachev, G. L. Yu, D. C. Elias, R. Jalil, A. A. Patel, A. Mishchenko, A. S. Mayorov, C. R. Woods, J. R. Wallbank, M. Mucha-Kruczynski, B. A. Piot, M. Potemski, I. V. Grigorieva, K. S. Novoselov, F. Guinea, V. I. Fal'ko, and A. K. Geim, *Nature*, **497**, 594 (2013).
- [6] D. J. Thouless, M. Kohmoto, M. P. Nightingale, and M. den Nijs, *Phys. Rev. Lett.*, **49**, 405 (1982).
- [7] D. Osadchy and J. E. Avron, *J. Math. Phys.*, **42**, 5665 (2001).
- [8] E. Mueller, *Phys. Rev. A*, **70**, 041603 (2004).
- [9] R. O. Umucalilar, H. Zhai, and M. Oktel, *Phys. Rev. Lett.*, **100**, 070402 (2008).
- [10] F. Gerbier and J. Dalibard, *New J. Phys.*, **12**, 033007 (2010).
- [11] A. R. Kolovsky, *EPL*, **93**, 20003 (2011).
- [12] C. E. Creffield and F. Sols, *EPL*, **101**, 40001 (2013).
- [13] M. Aidelsburger, M. Atala, S. Nascimbène, S. Trotzky, Y. A. Chen, and I. Bloch, *Phys. Rev. Lett.*, **107**, 255301 (2011).
- [14] M. Aidelsburger, M. Atala, S. Nascimbène, S. Trotzky, Y. A. Chen, and I. Bloch, *Appl. Phys. B* (2013).
- [15] D. Jaksch and P. Zoller, *New J. Phys.*, **5**, 56 (2003).
- [16] M. Aidelsburger, M. Atala, M. Lohse, J. T. Barreiro, B. Paredes, and I. Bloch, *arXiv*, **1308.0321** (2013).
- [17] H. Miyake, G. A. Siviloglou, C. J. Kennedy, W. C. Burton, and W. Ketterle, *arXiv*, **1308.1431** (2013).
- [18] E. Alba, X. Fernandez-Gonzalvo, J. Mur-Petit, J. K. Pachos, and J. J. Garcia-Ripoll, *Phys. Rev. Lett.*, **107**, 235301 (2011).
- [19] N. Goldman, J. Dalibard, A. Dauphin, F. Gerbier, M. Lewenstein, P. Zoller, and I. B. Spielman, *Proceedings of the National Academy of Sciences of the United States of America*, **110**, 6736 (2013).
- [20] D. A. Abanin, T. Kitagawa, I. Bloch, and E. Demler, *Phys. Rev. Lett.*, **110**, 165304 (2013).
- [21] L. Wang, A. A. Soluyanov, and M. Troyer, *Phys. Rev. Lett.*, **110**, 166802 (2013).
- [22] X.-J. Liu, K. T. Law, T. K. Ng, and P. A. Lee, *arXiv*, **1306.5223** (2013).
- [23] M. Jarrell and J. E. Gubernatis, *Physics Reports*, **269**, 133 (1996).
- [24] Y. Hasegawa, P. Lederer, T. M. Rice, and P. B. Wiegmann, *Phys. Rev. Lett.*, **63**, 907 (1989).
- [25] W. Xu, L. Yang, M. Qin, and T. Xiang, *Phys. Rev. B*, **78**, 241102 (2008).
- [26] L.-P. Yang, W.-H. Xu, M.-P. Qin, and T. Xiang, *J. Phys. Soc. Jpn.*, **81**, 044605 (2012).
- [27] N. Gemelke, X. Zhang, C.-L. Hung, and C. Chin, *Nature*, **460**, 995 (2009).
- [28] K. Van Houcke, F. Werner, E. Kozik, N. Prokof'ev, B. Svistunov, M. J. H. Ku, A. T. Sommer, L. W. Cheuk, A. Schirotzek, and M. W. Zwierlein, *Nature Physics*, **8**, 366 (2012).
- [29] M. J. H. Ku, A. T. Sommer, L. W. Cheuk, and M. W. Zwierlein, *Science*, **335**, 563 (2012).
- [30] Y.-R. Lee, M.-S. Heo, J.-H. Choi, T. T. Wang, C. A. Christensen, T. M. Rvachov, and W. Ketterle, *Phys. Rev. A*, **85**, 063615 (2012).
- [31] D. C. McKay and B. DeMarco, *Rep. Prog. Phys.*, **74**, 054401 (2011).
- [32] S. Fuchs, E. Gull, L. Pollet, E. Burovski, E. Kozik, T. Pruschke, and M. Troyer, *Phys. Rev. Lett.*, **106**, 030401 (2011).
- [33] A. W. Sandvik, *Phys. Rev. B*, **57**, 10287 (1998).
- [34] A. S. Mishchenko, N. V. Prokof'ev, A. Sakamoto, and Svistunov, BV, *Phys. Rev. B*, **62**, 6317 (2000).
- [35] K. S. D. Beach, *arXiv*, **cond-mat/0403055** (2004).
- [36] S. Fuchs, T. Pruschke, and M. Jarrell, *Phys. Rev. E*, **81**, 056701 (2010).
- [37] N. Prokof'ev and B. Svistunov, *arXiv*, **1304.5198** (2013).
- [38] R. N. Silver, D. S. Sivia, and J. E. Gubernatis, *Phys. Rev. B*, **41**, 2380 (1990).
- [39] Q. Zhou and T.-L. Ho, *Phys. Rev. Lett.*, **106**, 225301 (2011).
- [40] C. Sanner, E. J. Su, A. Keshet, R. Gommers, Y.-i. Shin, W. Huang, and W. Ketterle, *Phys. Rev. Lett.*, **105**, 040402 (2010).
- [41] T. Müller, B. Zimmermann, J. Meineke, J.-P. Brantut, T. Esslinger, and H. Moritz, *Phys. Rev. Lett.*, **105**, 040401 (2010).
- [42] T.-L. Ho and Q. Zhou, *Nature Physics*, **6**, 131 (2009).
- [43] P. N. Ma, L. Pollet, and M. Troyer, *Phys. Rev. A*, **82**, 033627 (2010).
- [44] L. Tarruell, D. Greif, T. Uehlinger, G. Jotzu, and T. Esslinger, *Nature*, **483**, 302 (2012).
- [45] G.-B. Jo, J. Guzman, C. K. Thomas, P. Hosur, A. Vishwanath, and D. M. Stamper-Kurn, *Phys. Rev. Lett.*, **108**, 045305 (2012).
- [46] B. Bauer et al, *J. Stat. Mech.: Theor. Exp.*, **2011**, P05001 (2011).
- [47] Other thermodynamic quantities like entropy and specific heat also reveal the DOS in the zero temperature limit, however unlike the compressibility, they are not directly accessible in the cold atom toolbox.
- [48] We need the local chemical potential in the trap to scan through the energy band, i.e. the density in the trap center to reach one. However, one can utilize the particle-hole symmetry of the Hofstadter lattice and only probe $\rho < 0.5$ to restore the whole spectrum.
- [49] μ_0 and α will vary in different experimental runs. One can nevertheless utilize the particle-hole symmetry of the Hofstadter model and chose the origin of chemical potential at $\rho = 0.5$ for each measurement.
- [50] For the spectral analysis calculation, we used the stochastic inference approach as implemented in [33] and the maximum entropy code implemented in the ALPS package [46]. We have enforced the particle-hole symmetry in the resulting DOS.
- [51] The LDA correction to the density profile is less than 0.1% [39] at the typical experimental temperatures ($T/J \sim 1$). We have also performed the deconvolution us-

ing the LDA density profiles. The images are only slightly different from the one using the exact density data, indicating the the LDA corrections to the final results are

indeed small. These corrections will further decreases if one uses a weaker trapping potential experimentally.